

Effect of Yb addition on strength and fracture toughness of Al-Zn-Mg-Cu-Zr aluminum alloy

ZHANG Zhuo(张 茁)¹, CHEN Kang-hua(陈康华)¹, FANG Hua-chan(方华婵)¹,
QI Xiong-wei(齐雄伟)¹, LIU Gang(刘 刚)²

1. State Key Laboratory of Powder Metallurgy, Central South University, Changsha 410083, China;
2. State Key Laboratory for Mechanical Behavior of Materials, Xi'an Jiaotong University, Xi'an 710049, China

Abstract: The effect of Yb addition on the strength and fracture toughness of Al-Zn-Mg-Cu-Zr aluminum alloy was investigated by measuring tensile properties and fracture toughness. The surface morphology was observed by optical microscopy, scanning electron microscopy and transmission electron microscopy. The results show that Yb addition can produce fine coherent Yb contained dispersoids. Those dispersoids trend to inhibit Al matrix recrystallization and retain the recovery deformed microstructure. Compared with Al-Zn-Mg-Cu-Zr alloy, Yb contained alloy demonstrates mechanical property improvements from 710 MPa to 747 MPa for ultimate strength, from 684 MPa to 725 MPa for yield strength, from 21 MPa·m^{1/2} to 29 MPa·m^{1/2} for fracture toughness with T6 treatment.

Key words: Al-Zn-Mg-Cu-Zr alloy; ytterbium; strength; fracture toughness; recrystallization

1 Introduction

Al-Zn-Mg-Cu series high-strength aluminum alloys with high specific strength and excellent mechanical properties have been the primary structural materials of aircraft in the space and ground transportation vehicles[1]. But the requirements for high yield stress and good fracture toughness are known to be contradictory[2–3]. This has hampered the extensive development and utilization of high-strength 7xxx series aluminum alloys. The relationships between microstructure and those two properties have been the focus of much research effort.

Adding trace elements to high-strength aluminum alloys can enhance their mechanical properties. It is found that trace elements and aluminum can form dispersoids to improve the recrystallization resistance of aluminum alloys[4–6], control the structure of grain boundary etc. These can stop cracks penetration along grain boundary[7–8]. Scandium is the most effective micro-alloying element in aluminum alloys. Scandium is sparingly soluble in aluminum in the solid state. At elevated temperatures, supersaturated solution

decomposes, to precipitate Al₃Sc (L1₂) phase. This phase of spherical particles can be very finely dispersed to improve strength for aluminum alloys. The effect can be enhanced by replacing partial Sc with Zr to produce Al₃(Sc,Zr) dispersoids to increase mechanical properties of aluminum alloys[9]. But expensive Sc addition is difficult to extensively apply[10]. The cheaper rare-earth elements are studied to replace Sc[11–12].

The present authors found that the addition of rare-earth element ytterbium, much cheaper than Sc, can enhance the recrystallization resistance and improve both strength and fracture toughness of Al-Zn-Mg-Cu-Zr alloy. Two patents have been generated[13–14]. In this work, the mechanism of the effect of ytterbium addition on strength and fracture toughness of Al-Zn-Mg-Cu-Zr alloy is investigated.

2 Experimental

Table 1 lists the nominal chemical composition of the experimental alloys. High purity elemental aluminum (99.9 %), magnesium (99.9 %), zinc (99%), and Al-Zr, Al-Cu, Al-Yb alloys as raw materials were smelted. The smelting temperature was kept at 700–740 °C and the

Table 1 Nominal chemical composition of studied alloys (mass fraction, %)

Alloy	Zn	Mg	Cu	Zr	Yb	Trace elements	Al
A-Zn-Mg-Cu-Zr	8.60	2.5	2.2	0.16	–	≤0.20	Bal.
Al-Zn-Mg-Cu-Zr-Yb	8.60	2.5	2.2	0.16	0.3	≤0.20	Bal.

metals were cast into $\phi 45$ mm ingot in graphite mould.

The cast ingots were homogeneously annealed at 465 °C for 24 h, then extruded at 410–430 °C into plate. The extrusion ratio used is 12.2. The extruded samples were held at 450 °C and 470 °C separately for 1 h, then kept at 485 °C for 2 h for stepped solution treatment, prior to quench into cold water. The samples were tempered at 130 °C for 24 h for artificial T6 treatment.

Tensile properties and fracture toughness were measured by a CSS-44100 testing machine. Volume electric conductivity was tested by a SX1931 digital micrometer (four-probe method).

The samples for optical microscopy observation were divided into two groups. One was anode coated after being electro-polished, and then the recrystallization behavior was observed by optical polarized microscopy (OM) on a Polyver-Met optical microscope. The second was etched with modified Keller reagent, and then the growth of subgrains was observed by OM. Thin foils for TEM observation were prepared by twin jet-polishing in electrolyte solution of nitric acid and methyl alcohol (1:3) and then examined on Tecnai G20 and H-800 transmission electron microscope. Fractography was examined on KYKY-2800 scanning electron microscope. Grain boundary character distributions was studied by EBSD.

3 Experimental results

3.1 Tensile properties

The tensile properties are displayed in Table 2. It can be seen that Yb addition can improve the mechanical property of Al-Zn-Mg-Cu-Zr alloy. The ultimate strength is increased from 710 MPa to 747 MPa, yield strength from 684 MPa to 725 MPa, and the elongation from 8.9% to 9.7%, respectively.

Table 2 Mechanical properties of studied alloys

Alloy	σ_b /MPa	$\sigma_{0.2}$ /MPa	δ /%
Al-Zn-Mg-Cu-Zr	710	684	8.9
Al-Zn-Mg-Cu-Zr-Yb	747	725	9.7

3.2 Fracture toughness

Table 3 lists the fracture toughness of the experimental alloys. It can be seen that Yb addition can improve the fracture toughness of Al-Zn-Mg-Cu-Zr alloys from 21 MPa·m^{1/2} to 29 MPa·m^{1/2}. The electric

conductivity is also improved by the addition of Yb. According to the relationship between electric conductivity and resistance to stress corrosion, SCC resistance of Al-Zn-Mg-Cu-Zr alloys can be improved to some degree with Yb addition. From Table 2 and Table 3, we can see that addition of Yb to Al-Zn-Mg-Cu-Zr alloy can enhance synthetical property of the alloy.

Table 3 Fracture toughness of studied alloys

Alloy	$K_{IC}(S-L)$ / (MPa·m ^{1/2})	Volume electric conductivity (IACS)/%
Al-Zn-Mg-Cu-Zr	21	28.6
Al-Zn-Mg-Cu-Zr-Yb	29	32.6

3.3 Microstructure

Fig.1 shows the optical microstructures of experimental alloys. The microstructures of hot extruded Al-Zn-Mg-Cu-Zr alloy and Al-Zn-Mg-Cu-Zr-Yb alloy maintain the fiber-like nonrecrystallization morphology (Figs.1(a) and (c)). It can be seen that the structures of Al-Zn-Mg-Cu-Zr alloy are composed of equiaxial grains and some of them begin to grow up after solution at 485 °C for 2 h (Fig.1(b)). Some recrystal grains appear after solution at 485 °C for 2 h, but the fiber-like nonrecrystallization morphology is still clearly discernible in grain structures of Al-Zn-Mg-Cu-Zr-Yb alloy (Fig.1(d)). The addition of Yb can enhance the recrystallization resistance of Al-Zn-Mg-Cu-Zr alloy.

Fig.2 shows EBSD maps and grain boundary character distributions of the studied alloys. From Figs.2(a) and (c), it can be seen that after solution treatment the grain boundary character distributions of Al-Zn-Mg-Cu-Zr alloy are mainly in high angle boundary of 25°–55°. From Figs.2(b) and (d), those of Al-Zn-Mg-Cu-Zr-Yb alloy are mainly in low angle boundary of 0°–20°. It is found that the transformation from the recovery deformed Al matrix to subgrain microstructures has been baffled by the addition of Yb and the addition of Yb can enhance the recrystallization resistance of Al-Zn-Mg-Cu-Zr alloy.

Fig.3 shows the TEM micrographs of T6-tempered samples. It can be seen from Figs.3(a)–(c) that spherical dispersoids coherent with the matrix disperse in the grain and at the grain boundary in Al-Zn-Mg-Cu-Zr-Cr-Yb alloy. The dispersoids contain Yb, Zr and Al according to EDX analysis. These fine spherical dispersoids of 10–30 nm uniformly disperse in the matrix and may be formed during the anneal treatment or hot-working processing.

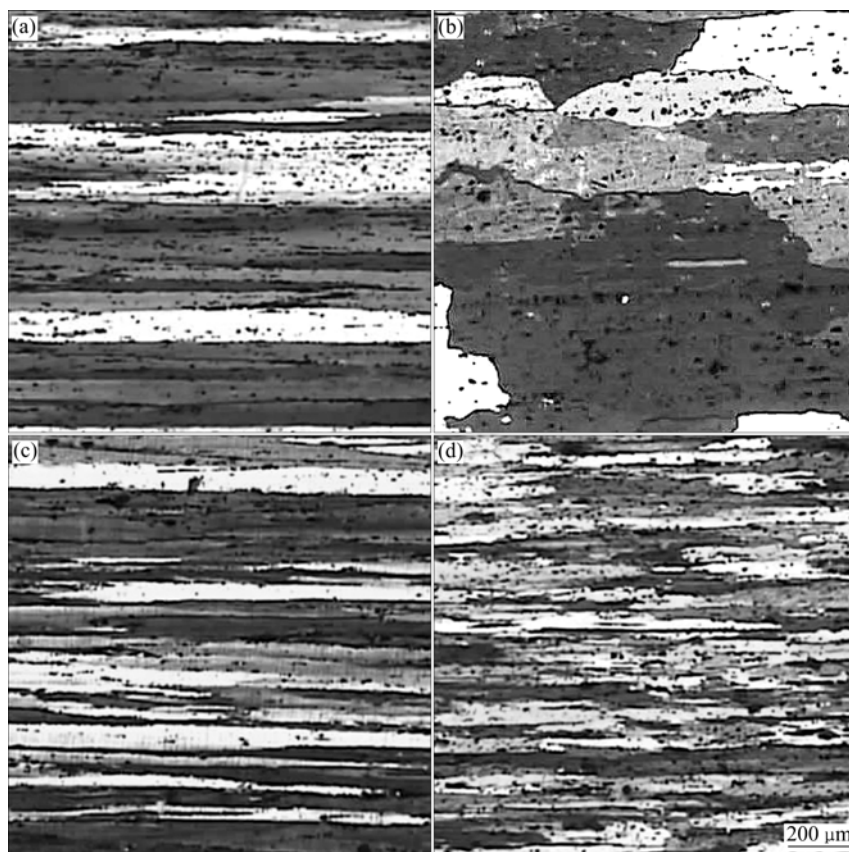


Fig.1 Optical micrographs of alloys at different annealing condition: (a) Al-Zn-Mg-Cu-Zr alloy in hot extruded condition; (b) Al-Zn-Mg-Cu-Zr alloy treated at 485 °C for 2 h; (c) Al-Zn-Mg-Cu-Zr-Yb alloy in hot extruded condition; (d) Al-Zn-Mg-Cu-Zr-Yb alloy treated at 485 °C for 2 h

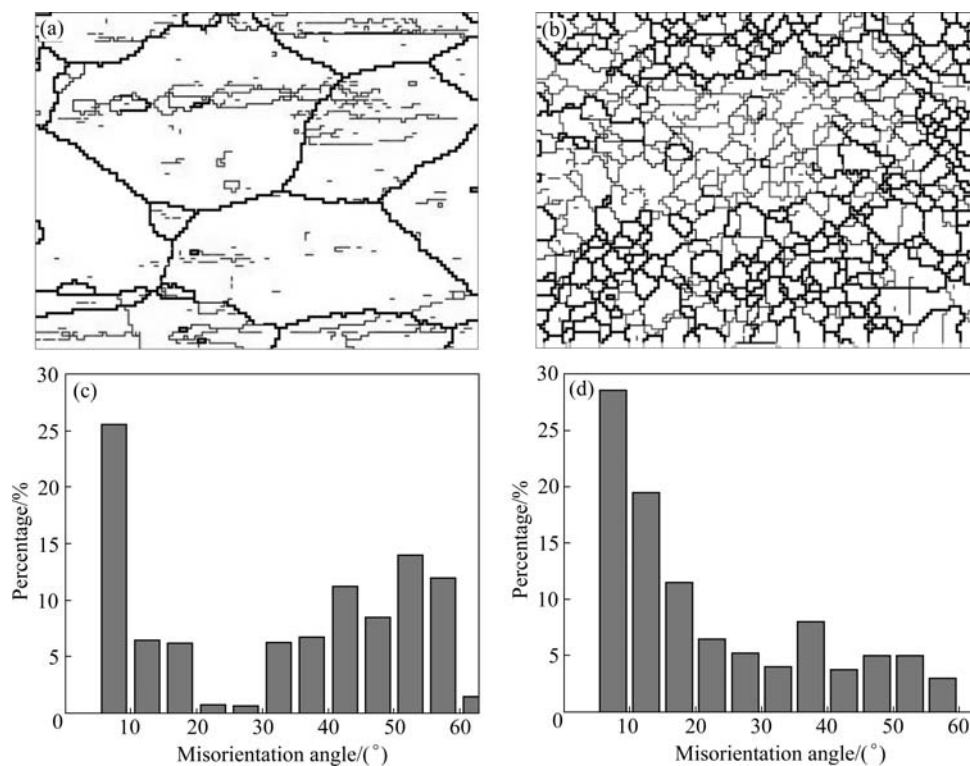


Fig.2 EBSD maps and grain boundary character distributions from EBSD maps: (a) EBSD map of Al-Zn-Mg-Cu-Zr alloy; (b) EBSD map of Al-Zn-Mg-Cu-Zr-Yb alloy; (c) Grain boundary character distributions of Al-Zn-Mg-Cu-Zr alloy; (d) Grain boundary character distributions of Al-Zn-Mg-Cu-Zr-Yb alloy

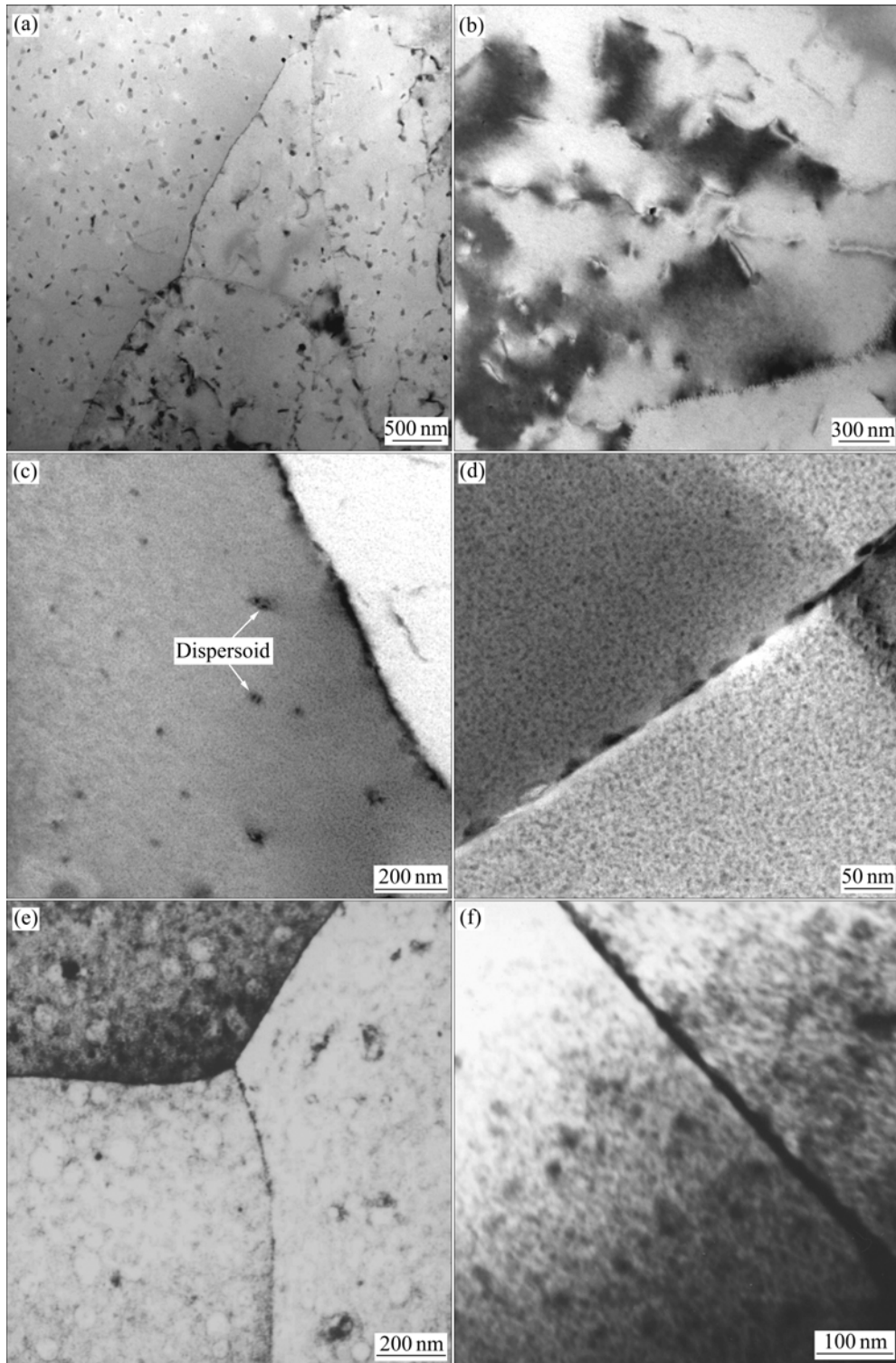


Fig.3 TEM bright-field images of T6-tempered alloys: (a)–(d) Al-Zn-Mg-Cu-Zr-Yb alloy; (e)–(f) Al-Zn-Mg-Cu-Zr alloy

They can pin dislocation and subgrain boundaries (Figs.3(a) and (b)) and therefore, inhibit subgrains growth and retain the recovery deformed Al matrix. As shown in Fig.3(d), the coarse and discontinuous equilibrium precipitates exist at the grain boundaries in the T6-tempered alloy. Around the grain boundaries there is narrow precipitate-free zone with width of 10 nm. By

contrast, continuous equilibrium precipitates exist at the grain boundaries in T6-tempered Al-Zn-Mg-Cu-Zr alloy, as shown in (Figs.3(e) and (f)).

3.4 Fractography

The images of fracture surface of T6-tempered samples are shown in Fig.4. The fractography of

Al-Zn-Mg-Cu-Zr alloy shows intergranular cracking. The dimple-type transgranular cracking dominates on the fracture surface of Al-Zn-Mg-Cu-Zr-Yb specimen. The number of the secondary cracks distributed on the grain and subgrain boundary is decreased.

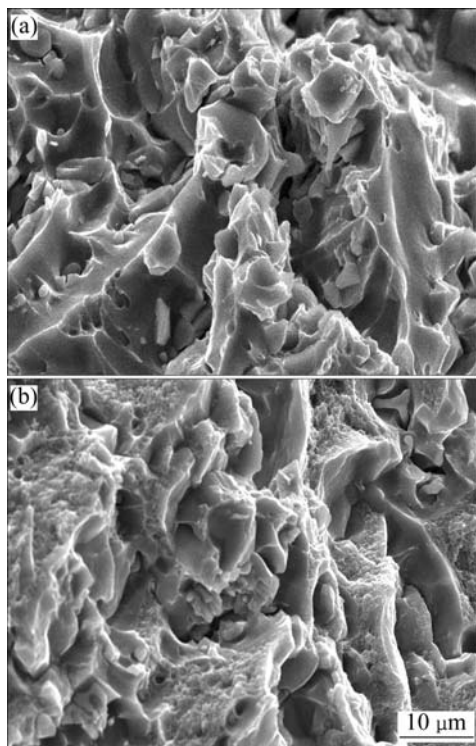


Fig.4 Fractographs of T6-tempered alloys: (a) Al-Zn-Mg-Cu-Zr; (b) Al-Zn-Mg-Cu-Zr-Yb

4 Discussion

4.1 Effect of Yb on inhibiting Al matrix recrystallization

The second dispersoids inhibit recrystallization when the interparticle distance λ and the particle diameter d is small ($\lambda < 1 \mu\text{m}$, $d \leq 0.3 \mu\text{m}$).

An estimation of the Zener drag, assuming a random spatial correlation between the boundaries and the dispersoids, is given by[15]

$$P_z = 3\phi\gamma GB/2r \quad (1)$$

where r is the radius and ϕ is the volume fraction of dispersoids. It shows that a high volume fraction of small dispersoids (large ϕ/r -ratio) is necessary in order to overcome the driving force for boundary migration and achieve high recrystallization resistance. The size of the fine spherical dispersoids containing Yb is approximately 10–30 nm and the distance between the dispersoids is also small (Fig.3(c)). This satisfies the condition of dispersoids hampering the recrystallization. Therefore, the dispersoids can strongly pin dislocation and subgrain boundaries. Consequently, they can restrict the

recombination of the dislocations and the movement of the subgrains (Fig.3(b)), effectively delay the recrystallization and enhance the recrystallization resistance of Al-Zn-Mg-Cu-Zr alloy.

4.2 Strengthening mechanism of Yb

Yb addition can improve the mechanical properties of Al-Zn-Mg-Cu-Zr alloy. The strengthening due to Yb addition mainly results from the dispersoid strengthening, fine-grain strengthening and dislocation strengthening.

1) Dispersoid strengthening

When dislocations have been inhibited by the Yb contained dispersoids in the slipping planes (Fig.3(b)), they will bypass the dispersoids through Orowan mechanism and leave dislocation loops behind. Those will induce reverse stress for the sources of dislocation and increase the moving resistance of the following dislocations and the flow stress. Consequently, they will lead to dispersoid strengthening effect.

According to Orowan dislocation strengthening, the strength increment is given by

$$\Delta\sigma_{y,or} = \frac{2Gb}{L_d} \quad (2)$$

where L_d is the interparticle spacing of dispersoids, G and b refer to the shear modulus of the matrix and Burger's vector of the dislocation.

Assuming that the dispersoids are uniformly distributed in the Al matrix in the form of cube, the interparticle spacing can be given by

$$L_d = 0.6d \left(\frac{2\pi}{\phi_d} \right)^{1/2} \quad (3)$$

where d is the diameter of the dispersoids, ϕ_d is the volume fraction of dispersoids.

2) Fine-grain strengthening

The Yb contained dispersoids can restrict recrystallization and inhibit the growth of grain, leading to fine-grain strengthening. According the standard Hall-Petch equation:

$$\Delta\sigma_{y,grain} = K \cdot d^{-1/2} \quad (4)$$

where d is the average grain size and K is a parameter that describes the relative strengthening contribution by grain boundaries. Clearly, the smaller the grain size, the higher the strength of the alloy. The fine dispersoids containing Yb can strongly inhibit recrystallization and the growth of subgrains. Therefore, the Al-Zn-Mg-Cu-Zr-Yb alloys maintain low-angle subgrains and lead to fine-grain strengthening.

3) Dislocation strengthening

High density dislocations in deformed microstructures could be reserved due to the dispersoids containing Yb pinning the dislocations and grain

boundaries strongly (Fig.3(b)). The movement of the dislocations will be blocked by the interaction between the moving dislocations. Partial of work-hardening strengthening is kept in Al-Zn-Mg-Cu-Zr-Yb alloy. The work-hardening strengthening is usually described by the Bailey-Hirsch relation[16]:

$$\Delta\sigma_{y, \text{ deformation}} = \alpha_2 G b \rho^{1/2} \quad (5)$$

The density of dislocations (ρ) has a linear relationship with the volume fraction of dispersoids (ϕ_d) ($\rho = \phi_d / (7.2\pi d^2)$).

4.3 Effect of Yb on fracture toughness

The extent of recrystallization has great effect on the fracture toughness of aluminum alloys. From the optical and TEM microstructures, it can be seen that the dispersoids containing Yb in Al-Zn-Mg-Cu-Zr-Yb alloy (Figs.3(b) and (c)) can inhibit the Al matrix recrystallization, and maintain the reverse deformed microstructures (Figs.2(b) and (d)). The reverse deformed small fiber-like nonrecrystallization microstructure is beneficial to improving fracture toughness of aluminum alloy.

The energy of low-angle boundaries in the reverse deformed microstructure is lower than that of high-angle boundaries. The aging precipitation at high-angle boundaries is much easier than that at low-angle boundaries. Due to grain boundary difference, discontinuous equilibrium precipitates exist at the grain boundaries of Al-Zn-Mg-Cu-Zr-Yb alloy (Fig.3(d)) and continuous equilibrium precipitates exist at the grain boundaries of Al-Zn-Mg-Cu-Zr alloy (Figs.3(e) and (f)). Contrast to the continuous precipitation, the discontinuous precipitation on grain boundary is beneficial to improving grain boundary fracture resistance and fracture toughness of aluminum alloy. Al-Zn-Mg-Cu-Zr-Yb alloy has higher fracture toughness than Al-Zn-Mg-Cu-Zr alloy because of different grain the boundary structure.

5 Conclusions

1) Yb addition to Al-Zn-Mg-Cu-Zr alloy can produce fine coherent dispersoids that can effectively pin the dislocations and subgrain boundaries, and enhance the resistance to recrystallization of Al-Zn-Mg-Cu-Zr alloy.

2) 0.3%Yb addition to Al-Zn-Mg-Cu-Zr alloy can improve the ultimate strength from 710 MPa to 747 MPa, yield strength from 684 MPa to 725 MPa, fracture

toughness from 21 MPa·m^{1/2} to 29 MPa·m^{1/2} with T6 treatment.

References

- [1] PAN Zhi-jun, LI Wen-xian. Current status and future trends of research on fracture toughness of high-strength aluminum alloys [J]. *Materials Review*, 2002, 16(7): 14–17.
- [2] LIU Wen-hui, ZHANG Xin-ming, LI Hui-jie, LIU Sheng-dan, HUANG Zhen-bao. Effect of solution on fracture toughness of 7A55 aluminum alloy [J]. *Journal of Central South University (Science and Technology)*, 2007, 38(1): 1–45.
- [3] LEE K Y, KIM O W. Stress intensity factor for sheet-reinforced and cracked plate subjected to remote normal stress [J]. *Eng Fract Mech*, 1998, 61(3): 461–466.
- [4] RYUM N. Precipitation and recrystallization in an Al-0.5%Zr alloy [J]. *Acta Metallurgica*, 1969, 17(3): 269–278.
- [5] YOSHIDA H, BABA Y. The role of zirconium to improve strength and stress-corrosion resistance of Al-Zn-Mg and Al-Zn-Mg-Cu alloys [J]. *Transactions of the Japan Institute of Metals*, 1982, 23(10): 620–630.
- [6] MUKHOPADHYAY A K, YANG Q B. The influence of zirconium on the early stages of aging of a ternary Al-Zn-Mg alloy [J]. *Acta Metall Mater*, 1994, 43(9): 3083–3091.
- [7] CHEN C Q, KNOTT J F. Effects of dispersoid particles on toughness of high-strength aluminum alloys [J]. *Metal Science*, 1981, 15(8): 357–364.
- [8] SHARMA M M, AMATEAU M F, EDEN T J. Hardening mechanisms of spray formed Al-Zn-Mg-Cu alloys with scandium and other elemental additions [J]. *Journal of Alloys and Compounds*, 2006, 416: 135–142.
- [9] DAI Xiao-yuan, XIA Chang-qing, LONG Chun-guang, PENG Xiao-min. Microstructure and properties of Al-9.0Zn-2.5Mg-1.2Cu-0.12Sc-0.15Zr alloy [J]. *The Chinese Journal of Nonferrous Metals*, 2007, 17(3): 396–401. (in Chinese)
- [10] NES E, RYUM N, HUNDERI O. The effect of precipitate on abnormal grain growth [J]. *Acta Metall*, 1985, 33(11): 156–200.
- [11] YANG Jun-jun, NIE Zuo-ren, JIN Tou-nan, RUAN Hai-qiong, ZUO Tie-yong. Form and refinement mechanism of element Er in Al-Zn-Mg alloy [J]. *The Chinese Journal of Nonferrous Metals*, 2004, 14(4): 620–626. (in Chinese)
- [12] KARNESKY R A, VAN DALEN M E, DUNAND D C, SEIDMAN D. Effects of substituting rare-earth elements for scandium in a precipitation-strengthened Al-0.08at%Sc alloy [J]. *Scripta Materialia*, 2006, 55(5): 437–440.
- [13] CHEN Kang-hua, FANG-Hua-chan, ZHANG Zhuo, ZHU Chang-jun, HUANG Lang-ping. High strength, high toughness and high corrosion resistant Al-Zn-Mg-(Cu) alloys. CN patent 200610136903.9 [P]. 2006–12–19.
- [14] CHEN Kang-hua, HUANG Lan-ping, FANG Hua-chan, ZHANG Zhuo. Anti-recrystallized Al-Zn-Mg-(Cu) alloys. CN 200610031119.0 [P]. 2006–01–09.
- [15] ASHBY M F. The interaction of crystal boundaries with second-phase particles [J]. *Transactions of the Metallurgical Society of AIME*, 1969, 245(8): 413–420.
- [16] BAILEY J E, HIRSCH P B. The dislocation distribution flow stress and stored energy in cold-worked polycrystalline silver [J]. *Philosophical Magazine*, 1960, 5(53): 485–497.

(Edited by YANG Bing)